Article:
Tai, K, Rappolt, M orcid.org/0000-0001-9942-3035, He, X et al. (6 more authors) (2019) Effect of β-sitosterol on the curcumin-loaded liposomes: Vesicle characteristics, physicochemical stability, in vitro release and bioavailability. Food Chemistry, 293. pp. 92-102. ISSN 0308-8146

https://doi.org/10.1016/j.foodchem.2019.04.077

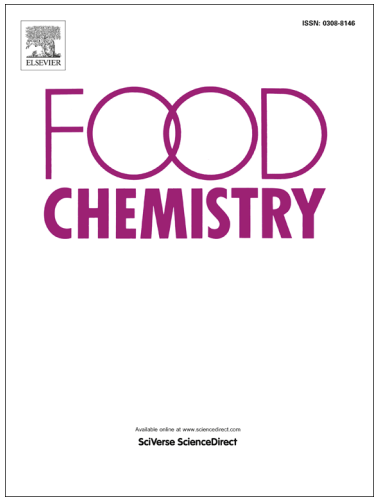

Effect of β-sitosterol on the curcumin-loaded liposomes: vesicle characteristics, physicochemical stability, *in vitro* release and bioavailability

Kedong Tai, Michael Rappolt, Xiaoye He, Yang Wei, Shaoxin Zhu, Jingbo Zhang, Like Mao, Yanxiang Gao, Fang Yuan

PII: S0308-8146(19)30741-1
DOI: https://doi.org/10.1016/j.foodchem.2019.04.077
Reference: FOCH 24678

To appear in: *Food Chemistry*

Received Date: 8 November 2018
Revised Date: 1 April 2019
Accepted Date: 22 April 2019

Please cite this article as: Tai, K., Rappolt, M., He, X., Wei, Y., Zhu, S., Zhang, J., Mao, L., Gao, Y., Yuan, F., Effect of β-sitosterol on the curcumin-loaded liposomes: vesicle characteristics, physicochemical stability, *in vitro* release and bioavailability, *Food Chemistry* (2019), doi: https://doi.org/10.1016/j.foodchem.2019.04.077

Effect of β-sitosterol on the curcumin-loaded liposomes: vesicle characteristics, physicochemical stability, in vitro release and bioavailability

Kedong Tai [a], Michael Rappolt [b], Xiaoye He [a], Yang Wei [a], Shaoxin Zhu [c], Jingbo Zhang [c], Like Mao [a], Yanxiang Gao [a], Fang Yuan [*,a]

[a] Beijing Advanced Innovation Center for Food Nutrition and Human Health, Beijing Laboratory for Food Quality and Safety, College of Food Science & Nutritional Engineering, China Agricultural University, Beijing 100083, P.R. China

[b] School of Food Science and Nutrition, University of Leeds, Leeds LS2 9JT, U.K.

[c] Guangdong Sino Nutri-food Biological Technology Co., Ltd., Dongguan 523000, P.R. China

* Corresponding author (Fang Yuan).

Tel: +86-10-62737034

Address: Box 112, No.17 Qinghua East Road, Haidian District, Beijing 100083, China

E-mail: yuanfang0220@cau.edu.cn

Abstract

In this work, the effect of β-sitosterol (Sito) on vesicle characteristics, physicochemical stability as well as the in vitro release and bioavailability of curcumin-loaded liposomes (Cur-LP) was studied. When 20-33 mol% of Sito was incorporated, encapsulation efficiency of curcumin was improved due to the high amount of liquid-ordered domains in membranes. At 50 mol% Sito a lower encapsulation efficiency was observed possibly due to membrane defects. The physical, thermal and photo stability of curcumin in liposomes were markedly improved with increasing the amount of Sito. First-order kinetics fitted best the curcumin release dynamics of Sito containing liposomes, clearly showing that sustained release improved with increasing amounts of Sito in liposomes. Simulated digestion studies suggested that Sito concentration of about 20 to 33 mol% improved the bioavailability of curcumin in liposomes. These study shows that Sito is an applicable and potential route in forming healthier cholesterol-free curcumin-loaded liposomes for functional supplements.

Keywords: Liposomes; β-sitosterol; Curcumin; Vesicle stability; Release profile

1. Introduction

Functional delivery system in the form of liposomes have been widely studied in fields of pharmaceutics, cosmetics and food, with desirable advantages such as enhanced biocompatibility, biodegradability, nontoxicity and non-immunogenicity (McClements, 2015). The typical structure of liposomes is lamellar vesicle with an internal water core surrounded by one or more concentric phospholipid bilayers into which hydrophilic, hydrophobic or amphiphilic bioactive compounds can be encapsulated. Apart from the improvement of delivery efficiency, the interaction between these embedded bioactive compounds in liposomes can synergistically facilitate efficacies in the human body after ingestion (Alavi, Haeri, & Dadashzadeh, 2017). Nevertheless, the main challenges for liposomes in commercial application are (ⅰ) the relatively bad physicochemical stability caused by thermodynamic instability, (ⅱ) undesired membrane fusions, and (ⅲ) phospholipids degradation can cause the disintegration of self-assembled bilayers and leakage of bioactive compounds from vesicles (Khanniri, Bagheripoor-Fallah, Sohrabvandi, Mortazavian, Khosravi-Darani, & Mohammad, 2016). Beside this, instability can be accelerated by the unfavorable environmental conditions like temperature fluctuations during manufacturing, transportation and storage, and finally by high electrolyte concentration during gastric secretion (Nguyen, Huang, Gauthier, Yang, & Wang, 2016). In recent years, considerable research efforts have been devoted to the preparation of stable and multifunctional liposomes, which would effectively avoid membrane fusion. (Nag &

Awasthi, 2013). There are mainly two efficient modification routes proved in stabilizing liposomes. One concerns the surface modification of vesicles. Hereby, one or more layers are attached to the vesicles surface by intermolecular interactions between phospholipids and modified molecules, applying (ⅰ) chitosan (Alavi, Haeri, & Dadashzadeh, 2017; Liu, Liu, Zhu, Gan, & Le, 2015) and its derivatives (Karewicz, Bielska, Loboda, Gzyl-Malcher, Bednar, Jozkowicz, et al., 2013; Li, Deng, Cai, Zhang, Wang, Li, et al., 2017), silica (Li, Zhang, Su, Feng, Long, & Chen, 2012), (ⅱ) proteins (Gomez-Mascaraque, Sipoli, de la Torre, & Lopez-Rubio, 2017), (ⅲ) hyaluronan (Manconi, Manca, Valenti, Escribano, Hillaireau, Fadda, et al., 2017), (ⅳ) sodium alginate (Liu, Liu, Ye, Peng, Wei, Liu, et al., 2016), and (ⅴ) pectin (Zhou, Liu, Zou, Liu, Liu, Liang, et al., 2014). The other strategy concerns a compositional change of liposomal bilayers by incorporating (ⅰ) polyethylene glycol (PEG) (Abe, Higashi, Watabe, Kobayashi, Limwikrant, Yamamoto, et al., 2015), (ⅱ) small molecule emulsifiers (Li, Peng, Chen, Zhu, Zou, Liu, et al., 2018; Tai, He, Yuan, Meng, Gao, & Yuan, 2017), and (ⅲ) sterols (Mannock, Lewis, McMullen, & McElhaney, 2010).

In this study, we have explored the use of sterol-stabilized vesicles in order to improve the delivery of curcumin (Cur). Cur is a hydrophobic polyphenol extracted from the rhizome of turmeric, and its biological activity has been demonstrated in a number of studies including anti-oxidational, anti-inflammatory, antimicrobial, anticancer and wound healing effects (Anand, Kunnumakkara, Newman, & Aggarwal,

2007; Maheshwari, Singh, Gaddipati, & Srimal, 2006). However, the poor physicochemical stability and bioavailability of curcumin severely limit its application in products, and thus, its delivery has attracted great attention. Recent experiments applying emulsions (Ma, Zeng, Tai, He, Yao, Hong, et al., 2017), colloidal particles (Sun, Xu, Mao, Wang, Yang, & Gao, 2017), gels (Geremias-Andrade, Souki, Moraes, & Pinho, 2017), microcapsule (Wang, Lu, Wu, & Lv, 2009) and liposomes (Niu, Wang, Chai, Chen, An, & Shen, 2012) have demonstrated improved efficacy for the delivery of curcumin. Nevertheless, compared with other carriers, liposomal system have been identified as a promising encapsulation method for curcumin. For instance, the gastrointestinal absorption and plasma antioxidant activity could be both improved, when curcumin was encapsulated into liposomes displaying a relatively high encapsulation efficiency of 68% (Takahashi, Uechi, Takara, Asikin, & Wada, 2009). However, inserted curcumin molecules do disturb the arrangement of phospholipids in bilayers, which takes a negative effect on the stability of liposomes. Although the surface modification method had been proved useful in the formation of stable curcumin-loaded liposomes (Li et al., 2018; Liu et al., 2015), the more complicated preparation procedure and enhanced number of parameters to be controlled, are not conducive for large-scale industrial processing. The safety of coating layer materials is indeed questionable in food products.

The incorporation of sterols increase the packing density of phospholipids in bilayers due to introduction of the liquid ordered phase (l_o), which displayed

phospholipids with an increased chain order, but at the same time the fluid state of the membranes is conserved (Rappolt et al., 2003). Increasing amount of Sito in phospholipid membranes leads to an increased membrane rigidity and consequently reduces its permeability (Hodzic et al., 2008). For this reason, cholesterol is frequently used in liposomal preparation acting as "rebars" reinforcing the membranes stability as described in our previous study (Tai, Liu, He, Ma, Mao, Gao, et al., 2018). Noteworthy, cholesterol is though also associated closely with cardiovascular diseases (Hokanson & Austin, 1996). Thus, the long-term intake of a considerable amount of cholesterol from liposomes products in dietary products is not advisable, especially for elderly. In our previous study, Sito also exhibited some stabilization capacities in blank liposomal membranes. Moreover, Sito is known as a "heart-friendly" phytosterol that does interfere with absorption of cholesterol (Kobayashi, Hamada, Goto, Imaizumi, & Ikeda, 2008), as well as shows positive anticancer effects by interfering on multiple cell signal pathways. In this respect the delivery of Sito through liposomes has shown to be health beneficial (Bin, Sayeed & Ameen, 2015), except for not following recommended dosages that might cause nausea, ingestion, gas or constipation (Ling & Jones, 1995), erectile dysfunction and reduced absorbency of Vitamin E.

It is a very practicable way to replace cholesterol with Sito in curcumin-loaded liposomes as long as the correct dosage of sterol is taken care of. The application of Sito in bioactive compounds-loaded liposomes has been reported rarely, especially for

curcumin-loaded liposomes (Cur-LP). In this study, Cur-LP with different concentrations of Sito (20, 25, 33 and 50 mol%) were prepared, and sterol-free one was used as a control. The vesicle size, encapsulation efficiency, morphology, membrane properties, physicochemical stability, in vitro releasing and bioavailability in simulated digestion were systematically investigated to characterize the Sito incorporated Cur-LP. Results of this study could be used as a reference for preparing phytosterol-modified liposomes in encapsulating hydrophobic bioactive compounds with enhanced physicochemical stability, as well as for the development of cholesterol-free liposomes.

2. Materials and methods

2.1. Materials

Lecigran 1000P (de-oiled, powdered soybean lecithin containing a mixture of phospho- and glycol-lipid, dispersible in water and partly soluble in ethanol) was obtained from Cargill Asia Pacific Food System Co., Ltd (Beijing, China). β-sitosterol was purchased from Aladdin biological technology Co., Ltd (Shanghai, China). Curcumin (> 95% purity) was obtained from Hebei Food Additive Co., Ltd (Hebei, China). Pyrene, 8-Anilino-1-naphthalene sulfonic acid (ANS) and 1,6-Diphenyl-1,3,5-hexatriene (DPH), mucin (M2378), pepsin (P7125, enzymatic activity ≥ 400 units/mg protein), pancreatin (P1750, 4 × USP), protamine (P4020) and bile salts were purchased from Sigma-Aldrich Chemical Co. (St. Louis, MO, USA). All other chemicals used in this study were analytical grade.

2.2. Preparation of curcumin-loaded liposomes

Cur-LP was prepared using the thin film hydration-high pressure homogenization method. Briefly, lecithin, Sito and curcumin were dissolved together in chloroform adequately. The concentrations of lecithin and curcumin were fixed at 10 mg/mL and 0.25 mg/mL, respectively while the concentration of Sito was ranged from 20 to 50 mol%. Organic solvent was vacuum-desiccated to form a thin lipid film using a rotary evaporator at 40 ℃. The further evaporating could remove residual chloroform as much as possible. Then, the coarse liposomes were formed by hydrating lipid film with phosphate buffer solution (PBS, 0.05 M, pH 7.0). Finally, Cur-LP was obtained by high-pressure homogenization at 50 MPa for three cycles. The Cur-LP without Sito (0 mol%) was prepared as a control.

2.3. Vesicle size and microstructure

Average vesicle size of Cur-LP was measured by dynamic light scattering using Malvern ZetasizerNano-ZS90 (Malvern Instruments Ltd., Worcestershire, UK) with a scattering angle of 90° and a refractive index of 1.490. The vesicle size was recorded from three independent measurements at 25 °C after 2 min of equilibration. In order to avoid multiple scattering, all samples were diluted 10-fold with PBS before measurements.

Transmission electron microscopy (TEM) was applied to observe microstructures of Cur-LP. One drop of diluted liposomes was placed onto a 200-mesh carbon coated copper grid and left for 2 min. After that, samples were negatively stained using

uranyl acetate solution (3%) for 90 s and air-dried at room temperature. When necessary, excess liquid was removed with filter paper. The treated Cur-LP was observed by JEM-1200EX TEM (Japanese Electronics Co., Ltd, Japan) at an accelerating voltage of 100 kV.

2.4. Encapsulation efficiency

The encapsulation efficiency (EE) of curcumin was measured using the protamine aggregation method according to our previous study (Tai, He, Yuan, Meng, Gao, & Yuan, 2017). Equal volumes of Cur-LP and protamine solution (10 mg/mL) were mixed and incubated for 6 h. Due to the strong electrostatic interaction caused by the opposite charges between liposomes and protamine, the Cur-LP could be easily separated by precipitation followed by a centrifugation step (10000 × g, 30 min) at 25 °C and supernatant was dissolved with anhydrous methanol. The amount of unencapsulated curcumin in the supernatant was determined by UV-vis spectrometer (UV-1800, Shimadzu Corporation, Japan) at 428 nm. The total amount of curcumin was determined by dissolving Cur-LP into anhydrous methanol sufficiently. The curcumin EE was calculated using the following equation:

$$EE(\%) = \frac{\text{Total amount of curcumin - Free amount of curcumin}}{\text{Total amount of curcumin}} \times 100 \quad (1)$$

2.5. Micropolarity of liposomal membranes

Because of pyrene's sensitivity to polarity changes in ith microenvironment, manifesting the degree of molecular order in membranes, the fluorescence characteristics of pyrene was used to probe the micropolarity of liposomal membranes

(Kalyanasundaram & Thomas, 1977). The diluted (10-fold) Cur-LP was mixed with a pyrene-acetone solution (2 mM) at a volume ratio of 50:1. The mixture was vortexed and incubated overnight at 4 °C. Fluorescence measurement was conducted at the excitation wavelength of 338 nm using F-7000 fluorescence spectrophotometer (Hitachi High-Technologies, Tokyo, Japan), the emission spectra were collected from 350 to 450 nm (scan speed was 240 nm/min, slit width was 5 nm). The fluorescence intensity ratio (I_1/I_3) of pyrene monomer vibronic peak 1 (I_1) and peak 3 (I_3) is closely related with the polarity around pyrene in bilayers. The high value of I_1/I_3 means the high micropolarity in membranes (Lemp, Zanocco, & Gunther, 2003).

2.6. Hydrophobicity of liposomal membranes

The diluted (10-fold) Cur-LP was mixed with ANS-PBS solution (8 mM) at a volume ratio of 50:1. The mixture was vortexed and incubated at room temperature for 30 min. Fluorescence measurement was conducted at the excitation wavelength of 350 nm, and the emission spectra were collected from 375 to 600 nm. Because of the high affinity of ANS to hydrophobic cavities and the same time with almost no fluorescent signal in aqueous environment, the recorded emission intensity reflect the amount of ANS up-take and manifest the degree of molecular order as well.

2.7. Fluidity of liposomal membranes

DPH probe the physical properties of the lipid chain region of the membrane. DPH movements are determined by measuring the degree to which DPH fluorescence emission is depolarized (Ionescu, Margină, Ilie, Iftime, & Ganea, 2013). Briefly, the

diluted (10-fold) Cur-LP was mixed with DPH solution (2 μM in dimethyl sulfoxide) at a volume ratio of 5:1. The fluorescence polarization of DPH was measured after incubation at room temperature for 60 min using fluorescence spectrophotometer equipped with excitation and emission polarization filters. The mixture was excited with vertically polarized light (360 nm), and the emission intensities were detected at 430 nm, including perpendicular and parallel to the excited light. The polarization (P) of DPH is inverse proportional to the fluidity of the membranes, which was calculated according to the following equations (Ionescu et al., 2013):

$$P = \frac{I_{0,0} - G\, I_{0,90}}{I_{0,0} + G\, I_{0,90}} \quad (2)$$

$$\text{with } G = I_{90,0} / I_{90,90} \quad (3)$$

where $I_{0,0}$ and $I_{0,90}$ as well as $I_{90,0}$ and $I_{90,90}$ are the fluorescence intensities of emitted light polarized parallel (0) and vertically (90), respectively. G is the grating correction coefficient. The emission fluorescence intensity of DPH in the aqueous phase is practically negligible.

2.8. Stability measurement

2.8.1. Storage stability

All Cur-LP were transferred into sealed brown glass bottles and stored at 4 °C for three weeks. The vesicle size of liposomes was detected at scheduled time intervals (0, 1, 2, 4, 7, 14, 21 d) during storage.

2.8.2. Thermal stability

The thermal stability of Cur-LP was investigated by recording the retention rate

of curcumin in liposomes after being heated. Samples were kept in a water bath at 60 °C for 30 min and 60 min, respectively, and cooled to room temperature immediately after. The stability of curcumin in Cur-LP without Sito and in PBS (Curcumin-PBS, a little Tween-80 was added to promote dissolution) were also tested for comparison under the same condition. The retention rate of curcumin was calculated according to the following equation:

$$\text{Retention Rate}(\%) = C_t / C_0 \times 100 \quad (4)$$

where C_0 and C_t represent concentrations of curcumin in the initial and at different sampling time in Cur-LP, respectively.

2.8.3. Photo stability

The photo stability of Cur-LP is essential due to the possible prolonged exposure to light during shelf life. All samples transferred into transparent glass tubes were subjected to simulated sunlight with an irradiance of 0.35 W/m^2 in a xenon test chamber (Q-SUN, Xe-1-B, Q-Lab Corporation, Ohio, USA) for 6 h. Taking sample once an hour and monitoring the concentration of curcumin in Cur-LP by absorbance. The retention rate of curcumin at different sampling time was determined with equation (4).

2.8.4. Physical stability

The physical stability of undiluted Cur-LP was performed by a multi-sample analytical centrifuge LUMiSizer® (LUM GmbH, Berlin, Germany), which detects the intensity of transmitted light as a function of time and position over the entire sample

length in rectangular test tubes (optical path was 2 mm). The variation of transmission profiles provides the information of the destabilization process of liposomes during centrifugation, including vesicle migration, coalescence and sedimentation caused by centrifugation. All samples were subjected to centrifugation at 4000 rpm for 1 h. The "instability index" was determined by using the SepView 6.0 software (LUM, Berlin, Germany), which is a dimensionless number between 0 (very stable) and 1 (very unstable).

2.9. In vitro release

The in vitro release profile of curcumin from Cur-LP was carried out using the dialysis membrane method according to the previous study with some modification (Wang, Liu, Xie, Zhang, & Gao, 2017). 5 mL of each sample was transferred into dialysis bag with 8000-12000 Da molecular weight cut-off. The dialysis bag was immersed into 100 mL of PBS containing 30% methanol and vibrated at room temperature. Methanol was added as a secondary solvent for curcumin. 5 mL of release medium was withdrawn and replaced with isopyknic fresh medium at scheduled time intervals (0.5, 1, 2, 4, 6, 8, 10, 12, 24, 36, 48 h). The concentration of curcumin in the release medium was measured by absorbance at 428 nm. The cumulative release (%) of curcumin was calculated by using the following equation:

$$\text{Cumulative release}(\%) = \sum_0^t \left(\frac{M_t}{M_0}\right) \times 100$$

where M_0 and M_t are amounts of curcumin in initial samples and the cumulative amount in releasing medium at each sampling time, respectively.

To understand in vitro release characteristic of curcumin from Sito incorporated liposomes better, four different models were applied to fit the obtained release data, i.e. concerning the (ⅰ) zero-order kinetics model (Najib & Suleiman, 1985), (ⅱ) first-order kinetics model (Desai, Singh, Simonelli, & Higuchi, 1966), (ⅲ) Higuchi model (Higuchi, 1963) and (ⅳ) Ritger-Peppas model (Korsmeyer, Gurny, Doelker, Buri, & Peppas, 1983) given in equations (6) to (9):

$$M_t / M_0 = kt \quad (6)$$

$$M_t / M_0 = 1-\exp(-kt) \quad (7)$$

$$M_t / M_0 = kt^{1/2} \quad (8)$$

$$M_t / M_0 = kt^n \quad (9)$$

where M_t / M_0 is the fraction of curcumin released from the sample at time t, k is the release constant of different models, n in the Ritger-Peppas model is the release exponent. The correlation coefficient (R^2) is calculated to illustrate the fitting degree between release model and data.

2.10. Simulated digestion

The simulated gastrointestinal tract (GIT) model was applied to evaluate the bioavailability of curcumin in liposomes. A simplified model simulating GIT including mouth, stomach and small intestine phase was established as described elsewhere (Li, et al., 2018) with some modifications. The whole digestion was conducted in water bath vibrator at 37 °C (DHSZ, Jiangsu taicang experimental equipment company, China). All solution need to be preheated at 37 °C before

mixing.

2.10.1. Mouth phase

The simulated saliva fluid (SSF) was prepared by dissolving NaCl (1.594 g), KCl (0.202 g) and mucin (0.6 g) into distilled water (1 L). The Cur-LP was mixed with SSF at a volume ratio of 1:1. The pH of simulated mouth phase was adjusted to 6.8 ± 0.1 and this digestion step took 10 min.

2.10.2. Stomach phase

The simulated gastric fluid (SGF) was prepared by dissolving NaCl (2 g), concentrated HCl (7 mL) and pepsin (3.2 g) into distilled water (1 L). Mixtures taken from simulated mouth phase were mixed with SGF at a volume ratio of 1:1. The pH of simulated stomach phase was adjusted to 1.5 approximately and this digestion step took 2 h.

2.10.3. Small intestine phase

The simulated intestinal fluid (SIF) was prepared by dissolving K_2HPO_4 (6.8 g), NaCl (8.775 g), bile salts (5 g) and pancreatin (3.2 g) into distilled water (1 L). Before the addition of SIF, the pH of mixtures taken from simulated stomach phase must be adjusted to 6.8 approximately, because the extremely acid environment could inactivate the pancreatin. Mixtures taken from simulated stomach phase were also mixed with SIF at a volume ratio of 1:1. The pH was adjusted to 7.0 and this digestion period took 2 h.

2.10.4. Bioavailability

When the simulated digestion procedure was completed, the raw digesta was rapidly cooled and centrifuged at 4°C for 30 min (10000×g). The supernatant was collected as this micellar fraction is expected to be easily absorbed by the intestinal epithelial cells, and hence represents the "bioavailable" fraction after digestion procedure. The concentration of curcumin in the supernatant was assayed by UV-vis spectrophotometer at 428 nm and calculated by calibration curve. The bioavailability (%) of curcumin was calculated using the following equation (Peng, Li, Zou, Liu, Liu & McClements, 2018a; Peng, Li, Zou, Liu, Liu & McClements, 2018b).:

$$\text{Bioavailability}(\%) = C_{Micelles} / C_{Initial} \times 100 \quad (10)$$

where $C_{Micelles}$ and $C_{Initial}$ represent concentrations of curcumin in the mixed micelles fraction and the initial sample without digestion, respectively

2.11. Statistical analysis

All experiments were conducted in triplicate and values were expressed as mean value ± standard deviation (SD). The results were statistically analyzed using SPSS software (IBM Corp., Chicago, IL, USA). Statistical significance was established at $p < 0.05$. Data were treated using Origin 9.0 (OriginLab Inc., Northampton, MA, USA).

3. Results and discussion

3.1. Vesicle characteristics of liposomes

The basic molecular structures between Sito and cholesterol are similar apart from an additional ethyl group at C_{24} in Sito. According to our previous study, Sito also had an obvious effect on liposomal vesicles when it was incorporated into blank

liposomes (Hodzic at al., 2008; Tai et al., 2018). The vesicle sizes of Cur-LP with different concentration of Sito changed the following: Cur-LP with 33 mol%, 25 mol% and 20 mol% of Sito were 194± 4 nm, 197 ± 2 nm and 197 ± 4 nm, respectively, which were significantly smaller than that of Sito-free Cur-LP (233± 11 nm). That is, Sito incorporation decreases the mean vesicle size of Cur-LP most likely due to reduced vesicle fusion after homogenization (Decker, Fahr, Kuntsche, & May, 2012). However, the largest vesicle size was obtained when 50 mol% of Sito was contained. The higher amount of Sito could evidently thicken liposomal membranes because of the over-loading and higher dimensional occupation. This consistent with results obtained by Cui, Wu, Hovgaard, Lu, Chen, & Qi (2015) who reported that the vesicle sizes of liposomes in the mass ratios of 4:1(about 160 nm) and 6:1 (about 140 nm) between phospholipid and ergosterol were significantly lower than that in the ratio of 2:1 (about 200 nm). It is worth noting that the highest vesicle size was formed when the lowest amount of ergosterol was incorporated (ratio of 8:1) in their study. In terms of molecular structure, the more complex structure of side chain in ergosterol that inserted into the hydrophobic area of bilayers against the formation of a stable state of membranes (Mannock, Lewis, McMullen, & McElhaney, 2010). Remarkably, the smallest and most stable vesicles are obtained in the miscibility gap of the phase diagram of sterol/lipid mixtures (Rappolt et al., 2003). Here the liquid disordered (l_d) and liquid ordered phases (l_o) coexist (20-33 mol% in this study), while vesicles in the purely disordered fluid phase (0 mol% Sito) and in the purely liquid ordered state (50

mol% Sito) are less stable and display a broader vesicle size distribution (cp. Fig. 1).

The encapsulation efficiency (EE) of curcumin in Sito incorporated Cur-LP improved significantly compared with the lower EE in Sito-free liposomes (Table 1). The highest EE was obtained when 33 mol% Sito was incorporated. However, for 50 mol% Sito containing vesicles the EE value decreased (73.2 ± 0.6%) and was similar with Sito-free ones. According to previous research, increasing the incorporated amount of Sito in membranes facilitated the encapsulation efficiency of oligopeptides in liposomes (Hwang, Tsai, & Hsu, 2010), which manifested that replacing cholesterol with Sito is feasible strategy for preparing oligopeptides-loaded liposomes with high EE. Concerning the lower EE for Cur-LP with 50 mol% Sito, it is tempting to assume that vesicles in the pure l_o-phase display too rigid membranes to form equally stable vesicles leading to the leakage of curcumin from the hydrophobic area of liposomes (Karn, Vanic, Pepic, & Skalko-Basnet, 2011).

To verify this notion, microstructures of all Cur-LP were observed using TEM (Fig. 1). At 20 to 33 mol% spherical to elliptical shaped vesicles are seen with a rather low size distribution (Fig. 1B-D). At 50 mol% Sito the situation is entirely different (Fig. 1A): ruptured vesicles, faceted vesicle as well as larger assemblies without any vesicular structure are visible. Similarly, without any Sito added (Fig. 1E), the vesicle size distribution is greatly enhanced and fused vesicles structures are visible. In the latter, larger vesicles may be caused by membranes fusion (high fluidity of the membranes is given), whereas for vesicles in the liquid ordered state the membranes

have the highest bending rigidity (Hodzic et al., 2008) and do not promote the formation of neat, stable vesicles. Likely, the increased bending rigidity of membranes in the l_o-phase lead to both, a reduced overall membrane curvature even on a macroscopic level and membrane defects are less likely to heal out in the absence of lipids in the liquid disordered (l_d) state. These phenomena are in good agreement with results of the bigger overall vesicle sizes and the lower EE values shown in Table 1. We note that some discrepancies of vesicle size results existed between TEM and DLS were apparent, but the overall trend is confirmed. TEM only catches the actual size in a certain area visually, while DLS calculates size in accordance with the diffusion speed of vesicles. Another factor concerns the recommended dilution process to avoid the influence of multiple light scattering in DLS analysis, which possibly changes the vesicle size distribution when compared with the primary sample (Tan, Feng, Zhang, Xia, & Xia, 2016). In order to complement the drawbacks given in DLS method in vesicle size measurement, TEM was additionally applied as an aid to give an overall perception of vesicle size and shape results, especially with respect to membranes fusion and vesicles aggregation.

3.2. Membrane properties of liposomes

3.2.1. Membrane micropolarity

The calculated fluorescence intensity ratios of I_1/I_3 and fluorescence spectra of pyrene were shown in Fig. 2A and S1, respectively, which had been used to investigate the polarity of microenvironment, where pyrene was located

(Kalyanasundaram & Thomas, 1977). The ratio of I_1/I_3 significantly decreased with increasing the amount of Sito incorporated in Cur-LP, which manifested that the fraction of hydrophilic domains was gradually decreased in bilayers. The liposomes modified by sucrose esters exhibited similar results when more sucrose esters were added (Lemp, Zanocco, & Gunther, 2003). Increasing amount of incorporated Sito increases the packing density of lipids (Yuba, Harada, Sakanishi, & Kono, 2011), which contributed to the more regular phospholipids arrangement. Hence, the denser hydrophobic environment, which has been verified by Hodzic et al. (2008) that the area per lipid and per acyl chain decreases with increasing sterol content, provides a tighter encapsulation area for hydrophobic curcumin molecules in bilayers.

3.2.2. Membrane hydrophobicity

ANS is used to evaluate the surface hydrophobicity of nano-carriers due to its strong affinity with hydrophobic cavities. According to the results in Fig. 2B and S2, the fluorescence intensity decreased gradually, when the more amount of Sito was incorporated. This indicates a decrease of hydrophobic cavities on the surface of membranes. It has been reported that the intermolecular interaction and hydrogen bonds formed between phospholipids and sterols restrained a deeper insertion of ANS into membranes, which demonstrated the formation of ordered structures on liposomal surfaces (Bui, Suga, & Umakoshi, 2016). That is, the ANS fluorescence intensity is lower in l_o-rich rafts compared with l_d-rich domains. Concluding, denser lipid packing in liposomal membranes caused by Sito, dose facilitate the encapsulation of curcumin

in liposomes, especially for Cur-LP with 33 mol%, 25 mol% and 20 mol% of Sito.

3.2.3. Membrane fluidity

Because of the non-polar and hydrophobic interactions, the liposomal membranes own the special fluidity like a cell. Fig. 2C shows the calculated values of polarization for different Cur-LP. The highest polarizations appeared in Cur-LP with 33 mol%, 25 mol% and 20 mol% of Sito. However, the relatively lower polarizations were obtained in Cur-LP with 50 mol% or 0 mol% of Sito added, which for the pure lipid system indicates a greater fluidity of the membranes. In contrast, the lower 50 mol% result is counterintuitive, since it is well known that membranes in purely liquid ordered state display the highest molecular packing density, less fluid membranes, increased membrane thicknesses and a reduced area per lipid (Hodzic et al., 2008). Although this is to be investigated in more details in the future, a plausible explanation of the low polarization value at 50 mol% Sito would be that DPH exhibits a lower partition coefficient in the pure l_o-phase due to its very dense molecular packing, when compared to the miscibility gap region, in which both l_o- and l_d- phase coexist. As previously reported, the fluidity of membranes similarly decreased, when cholesterol was incorporated into polyphenol-loaded liposomes, and the variation of polarization was insignificant when the concentration of sterol exceeded 20% (Ionescu, Margină, Ilie, Iftime, & Ganea, 2013). Additionally, the clearly greater number broken-up vesicles and non-vesicular assemblies (see Fig. 1A) may lead to a leaking out of both curcumin and DPH, which is supported by the low EE results of

curcumin in Cur-LP of 50 mol% Sito. To summarize, the encapsulation capacity of Sito incorporated liposomes was determined by comprehensive analysis of various membrane properties. The more ordered structures of membranes with lower fluidity (20-33 mol%) contributed to an improved encapsulation of curcumin into the hydrophobic area of liposomes.

3.3.Physicochemical stability

3.3.1. Storage stability

The storage stability was evaluated by monitoring vesicle sizes of liposomes in three weeks at 4°C (Table 1). The vesicle size of Sito-free Cur-LP increased from 233 ± 11 nm to 330 ± 12 nm after three weeks. Also the mechanical less-stable vesicles containing 50 mol% Sito displayed an increase from 383 ± 11 nm to 458 ± 7 nm. The prior vesicles have the most fluid membranes, which leads to easier membranes fusion and vesicles swelling phenomenon during storage (Abe, et al., 2015). For 50 mol% Sito, the poorly order vesicles and highly-defected non-vesicular assemblies shown in Fig. 1A, most probably increased in number over the time of storage accounting for the dramatic increase of measured particle size. Nonetheless, incorporating 20-33 mol% Sito effectively maintained the vesicle size of Cur-LP in storage.

3.3.2. Physical stability under centrifugation

The accelerated physical stability of liquid sample could be evaluated under centrifugation by the LUMiSizer®. The instability phenomenon related to vesicles migration was traced by the evolution of transmission profiles, a series of space- and

time-related transmission curves are shown in Fig. 3A. Red and green lines represented the earlier and later scanning times, respectively. The enhancement of transmission was attributed to the gradual deposition of vesicles subjected to a centrifugal force (Lei, Liu, Yuan, & Gao, 2014), and the different step-profile pattern represented the different migration speed of vesicles in Cur-LP (Caddeo, Manconi, Fadda, Lai, Lampis, Diez-Sales, et al., 2013). A similar transmission increase shown in Fig. 3A was also obtained by Tan et al. (2016), who investigated the stability of carotenoids-loaded liposomes. In contrast with the flat patterns for 0-33 mol% Sito incorporated specimens, the obvious stepwise pattern was obtained in 50 mol% Sito, is attributed to great heterogeneity of the sample (vesicles, defected vesicles and large non-vesicular assemblies coexist), which was confirmed by TEM and DLS.

To express the physical stability clearly, the instability index (compare section 2.8.4) is plotted in Fig. 3B. The instability index increased dramatically in the first ten minutes except for 50 mol% Sito incorporated Cur-LP. As the concentration of Sito increased, the slope of instability index curve declined. We conclude that increasing the amount of Sito improves the centrifugal stability of Cur-LP effectively.

3.3.3. Thermal stability

Fig. 3C depicted different retention rates of curcumin in Cur-LP subjected to heat treatment after 30 min and 60 min, respectively. In comparison to rapid degradation of curcumin in PBS that only 14% of curcumin retained after 30 min, Sito-free Cur-LP exhibited better thermal stability retaining more than 80% of curcumin after 30 min.

Moreover, the incorporation of Sito further suspended the degradation of curcumin in liposomes. When the concentration of Sito was increased up to 50 mol%, Cur-LP had the best thermal stability among these in first 30 min. The deeper embedding of curcumin in bilayers provided the better protection effect and made the less leakage of curcumin from Cur-LP, which is mainly attributed to denser molecular packing of the bilayers as well as the better ordered multi-lamellar vesicular structures (Fig. 1). The similar curcumin retention behavior reflects also in the alike vesicle size, structure and membrane fluidity for Sito-containing vesicles ranging from 20 to 33 mol%. However, the vesicle's stability was no longer conserved, when heating time reached to 60 min. Membrane structures were disrupted gradually in continuous heating, and there was no significance of retention rates between Cur-LP with different concentrations of Sito. Li et al. (2018) had investigated the thermal stability of pluronics modified Cur-LP and also found that there were no differences of thermal stability among different pluronics modified Cur-LP under longer heating conditions, which were better than Cur-LP without modification.

3.3.4. Photo stability

Daylight is an inevitable environmental stress for commercial products during their shelf life. Fig. 3D depicts the retention rate of curcumin in Cur-LP as a function of UV light processing time. Due to the lack of protection, curcumin in PBS was degraded rapidly, while a slower degradation trend was observed among Cur-LP. This indicates that the encapsulation capacity of liposomes can protect curcumin from the

influence of UV light to some extent. The improved photo stability of curcumin with increasing Sito concentrations may have different reasons: (ⅰ) due to the improved EE of curcumin less curcumin is exposed to UV light in the excess water phase, and (ⅱ) the tighter packing of curcumin deep inside the hydrophobic area of the bilayers diminishes the degradation drastically. For instance, the Cur-LP with 50 mol% of Sito had the best photo stability, which was also consistent with its best thermal stability under heating treatment for 30 min (Fig. 3C).

3.4. In vitro release study

The calculated cumulative release rates of Cur-LP plotted as a function of time at room temperature is shown in Fig. 4. There was a rapid increase of curcumin release during the first 6 h that is about 60% of curcumin was discharged for curcumin-PBS. However, Cur-LP exhibited a slower cumulative release, which was only about 20-30% of curcumin released after 6 h. When the concentration of Sito was increased in liposomes, even lower release rates were obtained for Cur-LP. Similarly, the release of sulforhodamine B-loaded liposomes was dramatically decreased with increasing the amounts of cholesterol in liposomes (Kaddah, Khreich, Kaddah, Charcosset, & Greige-Gerges, 2018). The increase of mechanical rigidity induced by the “condensing effect” or “ordering effect” of Sito (Saito & Shinoda, 2011), accompanied with the decrease of bilayers permeability, is likely to be responsible for this phenomenon that the release of curcumin from liposomes is prolonged. It was noticeable that the similar cumulative release profiles were obtained between 33 and

50 mol% Sito incorporated Cur-LP. As described in previous study, the release of sulforhodamine B was decreased, when the cholesterol content was 30 mol% or greater. In this case, a pure l_o-phase is formed, in which the tightly packed lipid chains restrict the release of curcumin form bilayers (Aguilar, Pino, Soto-Arriaza, Cuevas, Sánchez, & Sotomayor, 2012).

To further evaluate in detail the release mechanism of curcumin from Sito incorporated liposomes, zero-order, first-order, Higuchi and Ritger-Peppas models were used to manifest the release kinetics. Table 2 displays the fitted equations and correlation coefficients (R^2) of each model for different Cur-LP. The data for all curcumin samples which were fitted with first-order and Ritger-Peppas release models showed the highest correlation coefficients, and the first-order kinetics displaying the overall best fits (see R^2 values in Table 2 and Fig. 4). Generally, the release behavior largely depended on the diverse hydrophilic or hydrophobic properties of encapsulated compounds, as well as on the cohesiveness and continuity of liposomal membranes and the polymer coatings used as a physical barrier (Dong & Rogers, 1991). According to the release curves in Fig. 4, the diffusion-controlled mechanism are dominating the release behavior of curcumin from Sito incorporated liposomes, which is due to the lack of burst release phenomenon (Gibis, Ruedt, & Weiss, 2016). Besides, the fact that the correlation coefficient of each release model gradually reduced with the decrease of incorporated content of Sito, the diffusional exponent (n) (Ritger-Peppas model) was in the range from 0.223 to 0.303, which indicates that

Fickian diffusion dominated the diffusion mechanism of curcumin form Sito incorporated liposomes (Yang & Washington, 2006). Different results were obtained by Li et al. (2018) and Liu et al. (2015), who performed release studies with curcumin-loaded liposomes modified with pluronics and chitosan, respectively, where the diffusional exponents ranged from 0.45 to 0.89 indicating anomalous diffusion or non-Fickian diffusion. The coexistence of anomalous transport and Fickian diffusion is usually observed in drug release investigation, but the diffusional mass transport dominantly controls this process, and the diverse property of release medium (polarity or solubility) also plays an important role in the results of drug release study. In view of the strong hydrophobic property for curcumin, the existence of methanol could dissolve the curcumin into PBS release medium easier, which would be more practical than PBS alone with respect to an improved release profile. Although the incorporation of Sito was applied to change structural characteristics of liposomal membranes in this study, still the release data had fitted best with the first order kinetics (Fig. 4A). This is in agreement with Dash's conclusion that first-order models are more appropriate to describe the drug dissolution in pharmaceutical dosage (Dash, Murthy, Nath, & Chowdhury, 2010). The release results above can not only provide direct instruction for curcumin-loaded liposomes, but also provide research reference basis for hydrophobic flavonoid-loaded ones. When more in vivo studies are conducted, the sustained in vitro release results are of referenced value to some extent.

3.5. Simulated digestion study

After the simulated three-step GIT digestion, the bioavailability of curcumin in Sito incorporated liposomes was determined (see Table 1). It is well known that the absorption of nutrients by small intestinal epithelial cell is greatly attributed to the destructive effect of digestive enzymes and bile salts on nanocarriers (McClements, 2015). The available fraction of curcumin solubilized into the micellar phase induced by bile salts, gives a good indication for the overall bioavailability. In this study, bioavailabilities were over 50% for all Cur-LP. The Sito incorporated liposomes showed higher bioavailabilities apart from 50 mol% Sito case. On the one hand, the improved stability of Sito incorporated liposomes probably prevents curcumin from interacting with other chemicals in digestive juice as well as reduces the release and degradation of curcumin before intestinal digestion (Li, et al., 2018). On the other hand, the higher EE of curcumin contributes to deliver more amount of curcumin to the intestinal digestion. As discussed earlier, the highly rigid membranes of 50 mol% Sito incorporated Cur-LP (greater number of defected vesicles and larger non-vesicular assemblies coexist in Fig. 1A) does have a negative effect on the sustained release of curcumin from liposomes. Thus, in this case more curcumin might be exposed during the gastric digestion and rapidly destroyed by digestive enzymes before reaching intestinal digestion. Cheng et al. (2017) have studied different preparation methods for Cur-LP and bioavailability was only about 20%. The similar results were obtained by Li et al. (2018). Hence, the incorporation of Sito does improve the bioavailability of curcumin in liposomes as long as l_o- and l_d- phases

coexist in the membrane matrix, which deserves to be further studied for achieving even the better delivery of curcumin to the small intestine.

4. Conclusion

In this study, the Cur-LP combined with different concentrations of Sito were prepared successfully. The incorporation of Sito had a positive effect on improving the stability and bioavailability of Cur-LP. When the concentration of Sito ranged from 20 mol% to 33 mol%, the vesicle size stability in storage, encapsulation efficiency and bioavailability were significantly improved. For physical, thermal and photo stability, the improvement was obvious for Sito incorporated liposomes, while they would be best when the concentration of Sito up to 50 mol%. The stability performance of Cur-LP was closely related to the membranes characteristics like molecular arrangement and fluidity of bilayers. Excessive incorporation of Sito (50 mol%) was not conducive to the encapsulation of curcumin into liposomes as well as not beneficial for the bioavailability after simulated digestion. The in vitro release results of curcumin from Sito incorporated liposomes indicated Fickian diffusion mechanism and mostly followed first-order kinetic model. The usage of liposomes modified with Sito in this study provides a new strategy for curcumin encapsulated into liposomes with improved stability, higher bioavailability and controlled-release. This may be beneficial for the development of low-cholesterol liposomes with high nutritional value in the food industry.

Acknowledgments

This research was financially supported by the National Key R&D Program of China (2016YFD0400804, 2016YFD0400601) and National Natural Science Foundation of China (No. 31371836). We also acknowledge the financial support from the China Scholarship Council (CSC) for Mr. Tai's study in the United Kingdom.

References

Abe, K., Higashi, K., Watabe, K., Kobayashi, A., Limwikrant, W., Yamamoto, K., & Moribe, K. (2015). Effects of the PEG molecular weight of a PEG-lipid and cholesterol on PEG chain flexibility on liposome surfaces. Colloids and Surfaces a-Physicochemical and Engineering Aspects, 474, 63-70.

Aguilar, L. F., Pino, J. A., Soto-Arriaza, M. A., Cuevas, F. J., Sánchez, S., & Sotomayor, C. P. (2012). Differential dynamic and structural behavior of lipid-cholesterol domains in model membranes. PloS one, 7(6), e40254.

Alavi, S., Haeri, A., & Dadashzadeh, S. (2017). Utilization of chitosan-caged liposomes to push the boundaries of therapeutic delivery. Carbohydrate Polymers, 157, 991-1012.

Anand, P., Kunnumakkara, A. B., Newman, R. A., & Aggarwal, B. B. (2007). Bioavailability of Curcumin: Problems and Promises. Molecular Pharmaceutics, 4(6), 807-818.

Bin Sayeed, M. S., & Ameen, S. S. (2015). Beta-Sitosterol: A Promising but Orphan

Nutraceutical to Fight Against Cancer. Nutrition and Cancer-an International Journal, 67(8), 1214-1220.

Bui, T. T., Suga, K., & Umakoshi, H. (2016). Roles of Sterol Derivatives in Regulating the Properties of Phospholipid Bilayer Systems. Langmuir, 32(24), 6176-6184.

Caddeo, C., Manconi, M., Fadda, A. M., Lai, F., Lampis, S., Diez-Sales, O., & Sinico, C. (2013). Nanocarriers for antioxidant resveratrol: Formulation approach, vesicle self-assembly and stability evaluation. Colloids and Surfaces B-Biointerfaces, 111, 327-332.

Cheng, C., Peng, S., Li, Z., Zou, L., Liu, W., & Liu, C. (2017). Improved bioavailability of curcumin in liposomes prepared using a pH-driven, organic solvent-free, easily scalable process. RSC Advances, 7(42), 25978-25986.

Cui, M., Wu, W., Hovgaard, L., Lu, Y., Chen, D., & Qi, J. (2015). Liposomes containing cholesterol analogues of botanical origin as drug delivery systems to enhance the oral absorption of insulin. Int J Pharm, 489(1-2), 277-284.

Dash, S., Murthy, P. N., Nath, L., & Chowdhury, P. (2010). Kinetic Modeling on Drug Release from Controlled Drug Delivery Systems. Acta Poloniae Pharmaceutica, 67(3), 217-223.

Decker, C., Fahr, A., Kuntsche, J., & May, S. (2012). Selective partitioning of cholesterol and a model drug into liposomes of varying size. Chemistry and physics of lipids, 165(5), 520-529.

Desai, S. J., Singh, P., Simonelli, A. P., & Higuchi, W. I. (1966). Investigation of factors influencing release of solid drug dispersed in inert matrices. II. Quantitation of procedures. J Pharm Sci, 55(11), 1224-1229.

Dong, C., & Rogers, J. A. (1991). Polymer-Coated Liposomes - Stability and Release of Asa from Carboxymethyl Chitin-Coated Liposomes. Journal of Controlled Release, 17(3), 217-224.

Geremias-Andrade, I. M., Souki, N. P. D. B. G., Moraes, I. C. F., & Pinho, S. C. (2017). Rheological and mechanical characterization of curcumin-loaded emulsion-filled gels produced with whey protein isolate and xanthan gum. Lwt-Food Science and Technology, 86, 166-173.

Gibis, M., Ruedt, C., & Weiss, J. (2016). In vitro release of grape-seed polyphenols encapsulated from uncoated and chitosan-coated liposomes. Food Research International, 88, 105-113.

Gomez-Mascaraque, L. G., Sipoli, C. C., de la Torre, L. G., & Lopez-Rubio, A. (2017). Microencapsulation structures based on protein-coated liposomes obtained through electrospraying for the stabilization and improved bioaccessibility of curcumin. Food Chemistry, 233, 343-350.

Higuchi, T. (1963). Mechanism of sustained- action medication. Theoretical analysis of rate of release of solid drugs dispersed in solid matrices. J Pharm Sci, 52(12), 1145-1149.

Hodzic, A., Rappolt, M., Amenitsch, H., Laggner, P., & Pabst, G. (2008). Differential

modulation of membrane structure and fluctuations by plant sterols and cholesterol. Biophysical journal, 94(10), 3935-3944.

Hokanson, J. E., & Austin, M. A. (1996). Plasma triglyceride level is a risk factor for cardiovascular disease independent of high-density lipoprotein cholesterol level: a meta-analysis of population-based prospective studies. J Cardiovasc Risk, 3(2), 213-219.

Hwang, J. S., Tsai, Y. L., & Hsu, K. C. (2010). The feasibility of antihypertensive oligopeptides encapsulated in liposomes prepared with phytosterols-b-sitosterol or stigmasterol (vol 43, pg 133, 2010). Food Research International, 43(4), 1219-1219.

Ionescu, D., Margină, D., Ilie, M., Iftime, A., & Ganea, C. (2013). Quercetin and epigallocatechin-3-gallate effect on the anisotropy of model membranes with cholesterol. Food and Chemical Toxicology, 61, 94-100.

Kaddah, S., Khreich, N., Kaddah, F., Charcosset, C., & Greige-Gerges, H. (2018). Cholesterol modulates the liposome membrane fluidity and permeability for a hydrophilic molecule. Food and Chemical Toxicology, 113, 40-48.

Kalyanasundaram, K., & Thomas, J. K. (1977). Environmental Effects on Vibronic Band Intensities in Pyrene Monomer Fluorescence and Their Application in Studies of Micellar Systems. Journal of the American Chemical Society, 99(7), 2039-2044.

Karewicz, A., Bielska, D., Loboda, A., Gzyl-Malcher, B., Bednar, J., Jozkowicz, A.,

Dulak, J., & Nowakowska, M. (2013). Curcumin-containing liposomes stabilized by thin layers of chitosan derivatives. Colloids and Surfaces B-Biointerfaces, 109, 307-316.

Karn, P. R., Vanic, Z., Pepic, I., & Skalko-Basnet, N. (2011). Mucoadhesive liposomal delivery systems: the choice of coating material. Drug Development and Industrial Pharmacy, 37(4), 482-488.

Khanniri, E., Bagheripoor-Fallah, N., Sohrabvandi, S., Mortazavian, A. M., Khosravi-Darani, K., & Mohammad, R. (2016). Application of Liposomes in Some Dairy Products. Critical Reviews in Food Science and Nutrition, 56(3), 484-493.

Kobayashi, M., Hamada, T., Goto, H., Imaizumi, K., & Ikeda, I. (2008). Comparison of effects of dietary unesterified and esterified plant sterols on cholesterol absorption in rats. J Nutr Sci Vitaminol (Tokyo), 54(3), 210-214.

Korsmeyer, R. W., Gurny, R., Doelker, E., Buri, P., & Peppas, N. A. (1983). Mechanisms of Solute Release from Porous Hydrophilic Polymers. International Journal of Pharmaceutics, 15(1), 25-35.

Lei, F., Liu, F. G., Yuan, F., & Gao, Y. X. (2014). Impact of chitosan-EGCG conjugates on physicochemical stability of beta-carotene emulsion. Food Hydrocolloids, 39, 163-170.

Lemp, E., Zanocco, A. L., & Gunther, G. (2003). Structural changes in DODAC unilamellar liposomes by addition of sucrose esters monitored by using

fluorescent techniques. Colloids and Surfaces A-Physicochemical and Engineering Aspects, 229(1-3), 63-73.

Li, C., Zhang, Y., Su, T. T., Feng, L. L., Long, Y. Y., & Chen, Z. B. (2012). Silica-coated flexible liposomes as a nanohybrid delivery system for enhanced oral bioavailability of curcumin. International Journal of Nanomedicine, 7, 5995-6002.

Li, R. W., Deng, L., Cai, Z. W., Zhang, S. Y., Wang, K., Li, L. H., Ding, S., & Zhou, C. R. (2017). Liposomes coated with thiolated chitosan as drug carriers of curcumin. Materials Science & Engineering C-Materials for Biological Applications, 80, 156-164.

Li, Z. L., Peng, S.-F., Chen, X., Zhu, Y.-Q., Zou, L.-Q., Liu, W., & Liu, C.-M. (2018). Pluronics modified liposomes for curcumin encapsulation: Sustained release, stability and bioaccessibility. Food research international, 108, 246-253.

Ling, W. H., & Jones, P. J. H. (1995). Dietary phytosterols: a review of metabolism, benefits and side effects. Life sciences, 57(3), 195-206.

Liu, W. L., Liu, W., Ye, A. Q., Peng, S. F., Wei, F. Q., Liu, C. M., & Han, J. Z. (2016). Environmental stress stability of microencapsules based on liposomes decorated with chitosan and sodium alginate. Food Chemistry, 196, 396-404.

Liu, Y. J., Liu, D. D., Zhu, L., Gan, Q., & Le, X. Y. (2015). Temperature-dependent structure stability and in vitro release of chitosan-coated curcumin liposome. Food Research International, 74, 97-105.

Ma, P. H., Zeng, Q. H., Tai, K. D., He, X. Y., Yao, Y. Y., Hong, X. F., & Yuan, F. (2017). Preparation of curcumin-loaded emulsion using high pressure homogenization: Impact of oil phase and concentration on physicochemical stability. Lwt-Food Science and Technology, 84, 34-46.

Maheshwari, R. K., Singh, A. K., Gaddipati, J., & Srimal, R. C. (2006). Multiple biological activities of curcumin: A short review. Life Sciences, 78(18), 2081-2087.

Manconi, M., Manca, M. L., Valenti, D., Escribano, E., Hillaireau, H., Fadda, A. M., & Fattal, E. (2017). Chitosan and hyaluronan coated liposomes for pulmonary administration of curcumin. International Journal of Pharmaceutics, 525(1), 203-210.

Mannock, D. A., Lewis, R. N., McMullen, T. P., & McElhaney, R. N. (2010). The effect of variations in phospholipid and sterol structure on the nature of lipid-sterol interactions in lipid bilayer model membranes. Chemistry and Physics of Lipids, 163(6), 403-448.

McClements, D. J. (2015). Nanoscale Nutrient Delivery Systems for Food Applications: Improving Bioactive Dispersibility, Stability, and Bioavailability. Journal of Food Science, 80(7), N1602-N1611.

Nag, O., & Awasthi, V. (2013). Surface Engineering of Liposomes for Stealth Behavior. Pharmaceutics, 5(4), 542.

Najib, N., & Suleiman, M. S. (1985). The Kinetics of Drug Release from

Ethylcellulose Solid Dispersions. Drug Development and Industrial Pharmacy, 11(12), 2169-2181.

Nguyen, T. X., Huang, L., Gauthier, M., Yang, G., & Wang, Q. (2016). Recent advances in liposome surface modification for oral drug delivery. Nanomedicine, 11(9), 1169-1185.

Niu, Y. M., Wang, X. Y., Chai, S. H., Chen, Z. Y., An, X. Q., & Shen, W. G. (2012). Effects of Curcumin Concentration and Temperature on the Spectroscopic Properties of Liposomal Curcumin. Journal of Agricultural and Food Chemistry, 60(7), 1865-1870.

Peng, S., Li, Z., Zou, L., Liu, W., Liu, C., & McClements, D. J. (2018a). Enhancement of Curcumin Bioavailability by Encapsulation in Sophorolipid-Coated Nanoparticles: An in Vitro and in Vivo Study. Journal of agricultural and food chemistry, 66(6), 1488-1497.

Peng, S., Li, Z., Zou, L., Liu, W., Liu, C., & McClements, D. J. (2018b). Improving curcumin solubility and bioavailability by encapsulation in saponin-coated curcumin nanoparticles prepared using a simple pH-driven loading method. Food & function, 9(3), 1829-1839.

Rappolt, M., Vidal, M., Kriechbaum, M., Steinhart, M., Amenitsch, H., Bernstorff, S., & Laggner, P. (2003). Structural, dynamic and mechanical properties of POPC at low cholesterol concentration studied in pressure/temperature space. European Biophysics Journal, 31(8), 575-585.

Saito, H., & Shinoda, W. (2011). Cholesterol effect on water permeability through DPPC and PSM lipid bilayers: a molecular dynamics study. J Phys Chem B, 115(51), 15241-15250.

Sun, C. X., Xu, C. Q., Mao, L. K., Wang, D., Yang, J., & Gao, Y. X. (2017). Preparation, characterization and stability of curcumin-loaded zein-shellac composite colloidal particles. Food Chemistry, 228, 656-667.

Tai, K., Liu, F., He, X., Ma, P., Mao, L., Gao, Y., & Yuan, F. (2018). The effect of sterol derivatives on properties of soybean and egg yolk lecithin liposomes: Stability, structure and membrane characteristics. Food Research International, 109, 24-34.

Tai, K. D., He, X. Y., Yuan, X. D., Meng, K., Gao, Y. X., & Yuan, F. (2017). A comparison of physicochemical and functional properties of icaritin-loaded liposomes based on different surfactants. Colloids and Surfaces A-Physicochemical and Engineering Aspects, 518, 218-231.

Takahashi, M., Uechi, S., Takara, K., Asikin, Y., & Wada, K. (2009). Evaluation of an Oral Carrier System in Rats: Bioavailability and Antioxidant Properties of Liposome-Encapsulated Curcumin. Journal of Agricultural and Food Chemistry, 57(19), 9141-9146.

Tan, C., Feng, B., Zhang, X. M., Xia, W. S., & Xia, S. Q. (2016). Biopolymer-coated liposomes by electrostatic adsorption of chitosan (chitosomes) as novel delivery systems for carotenoids. Food Hydrocolloids, 52, 774-784.

Wang, M., Liu, M., Xie, T. T., Zhang, B. F., & Gao, X. L. (2017). Chitosan-modified cholesterol-free liposomes for improving the oral bioavailability of progesterone. Colloids and Surfaces B-Biointerfaces, 159, 580-585.

Wang, Y., Lu, Z. X., Wu, H., & Lv, F. X. (2009). Study on the antibiotic activity of microcapsule curcumin against foodborne pathogens. International Journal of Food Microbiology, 136(1), 71-74.

Yang, S., & Washington, C. (2005). Drug release from microparticulate systems (pp. 183-211). New York: Taylor & Francis.

Yuba, E., Harada, A., Sakanishi, Y., & Kono, K. (2011). Carboxylated hyperbranched poly(glycidol)s for preparation of pH-sensitive liposomes. Journal of Controlled Release, 149(1), 72-80.

Zhou, W., Liu, W., Zou, L. Q., Liu, W. L., Liu, C. M., Liang, R. H., & Chen, J. (2014). Storage stability and skin permeation of vitamin C liposomes improved by pectin coating. Colloids and Surfaces B-Biointerfaces, 117, 330-337.

Figure Captions & Figures

Fig. 1. TEM images of curcumin-loaded liposomes combined with different amounts of β-sitosterol. (A) 50 mol%, (B) 33 mol%, (C) 25 mol%, (D) 20 mol%, (E) 0 mol%. Scale bars are 200 nm.

Fig. 2. Membrane characteristics of curcumin-loaded liposomes with different concentrations of β-sitosterol were investigated by pyrene (A), ANS (B) and DPH (C) at 25℃, respectively. Error bars represent standard deviations.

Fig. 3. The stability of curcumin-loaded liposomes with different concentrations of β-sitosterol were evaluated in there aspects: the physical centrifugation stability was determined by transmission profile (A) and instability index curve (B) using LUMiSizer®, thermal stability at 60℃ for 30 and 60 min (C) and photo stability under UV light with an irradiance of 0.35 W/m^2 (D), respectively. Error bars represent standard deviations.

Fig. 4. In vitro release model curves of curcumin from liposomes with different concentrations of β-sitosterol at room temperature during 48 h. Release model equation refer to first-order (A), Higuchi (B), Ritger-Peppas (C) and zero-order (D) kinetics, respectively. Error bars represent standard deviations.

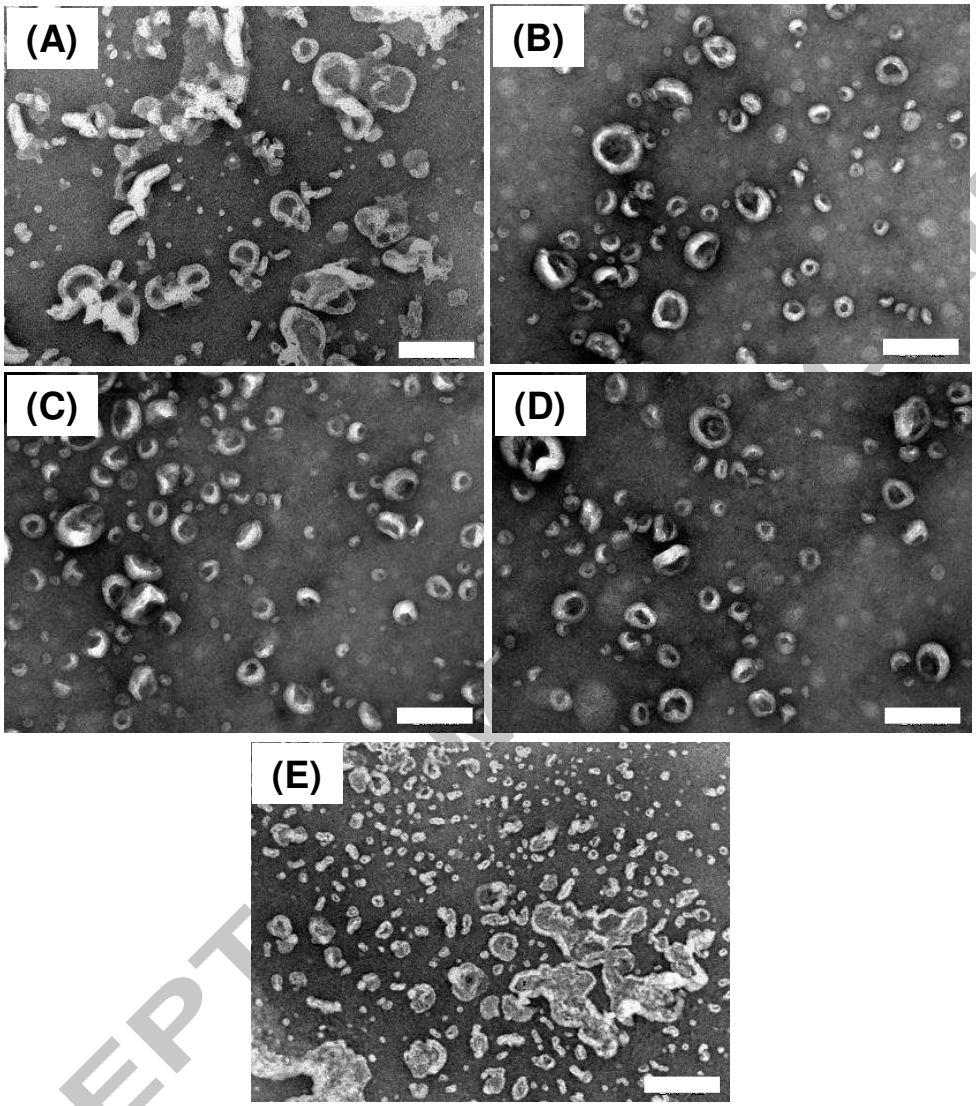

Fig. 1

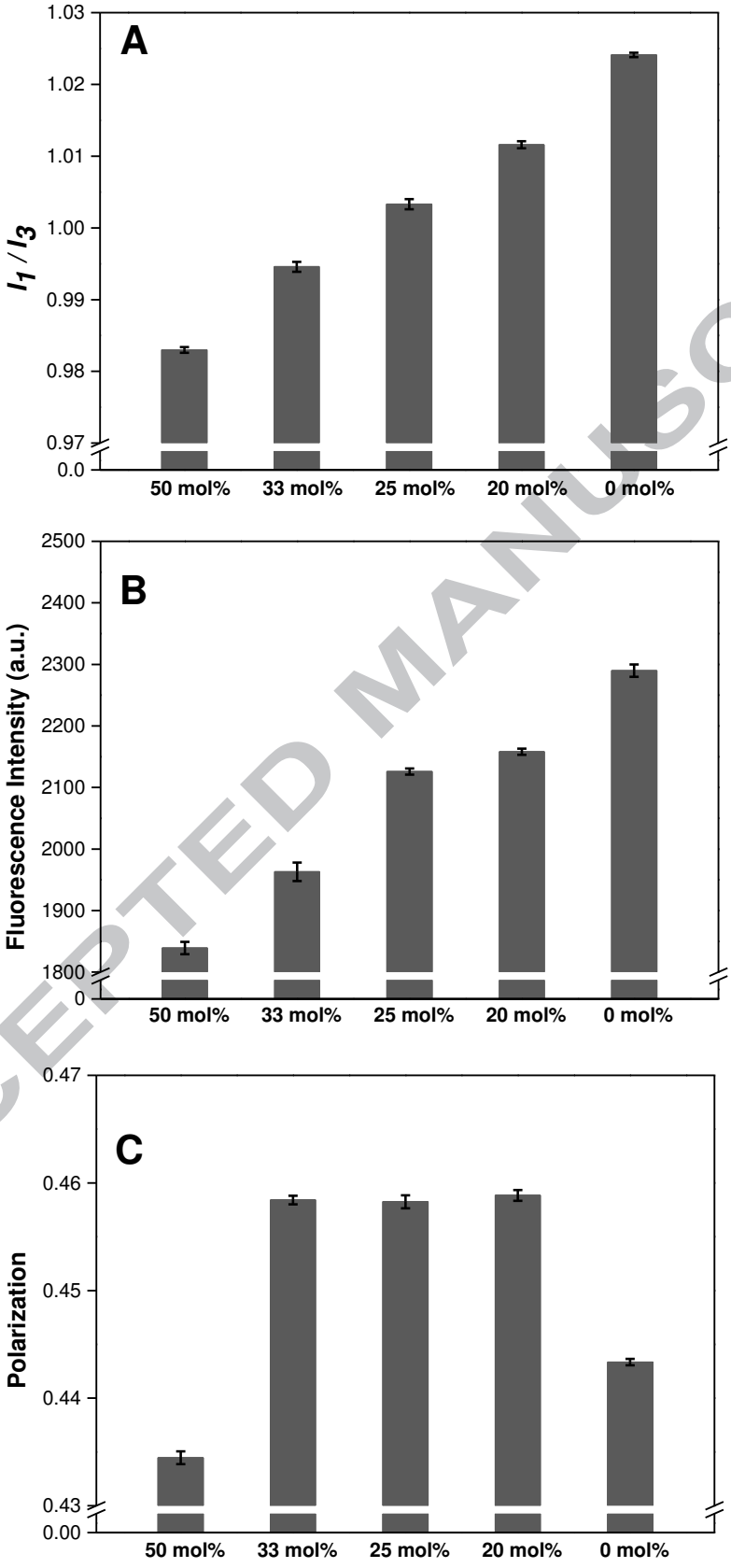

Fig. 2

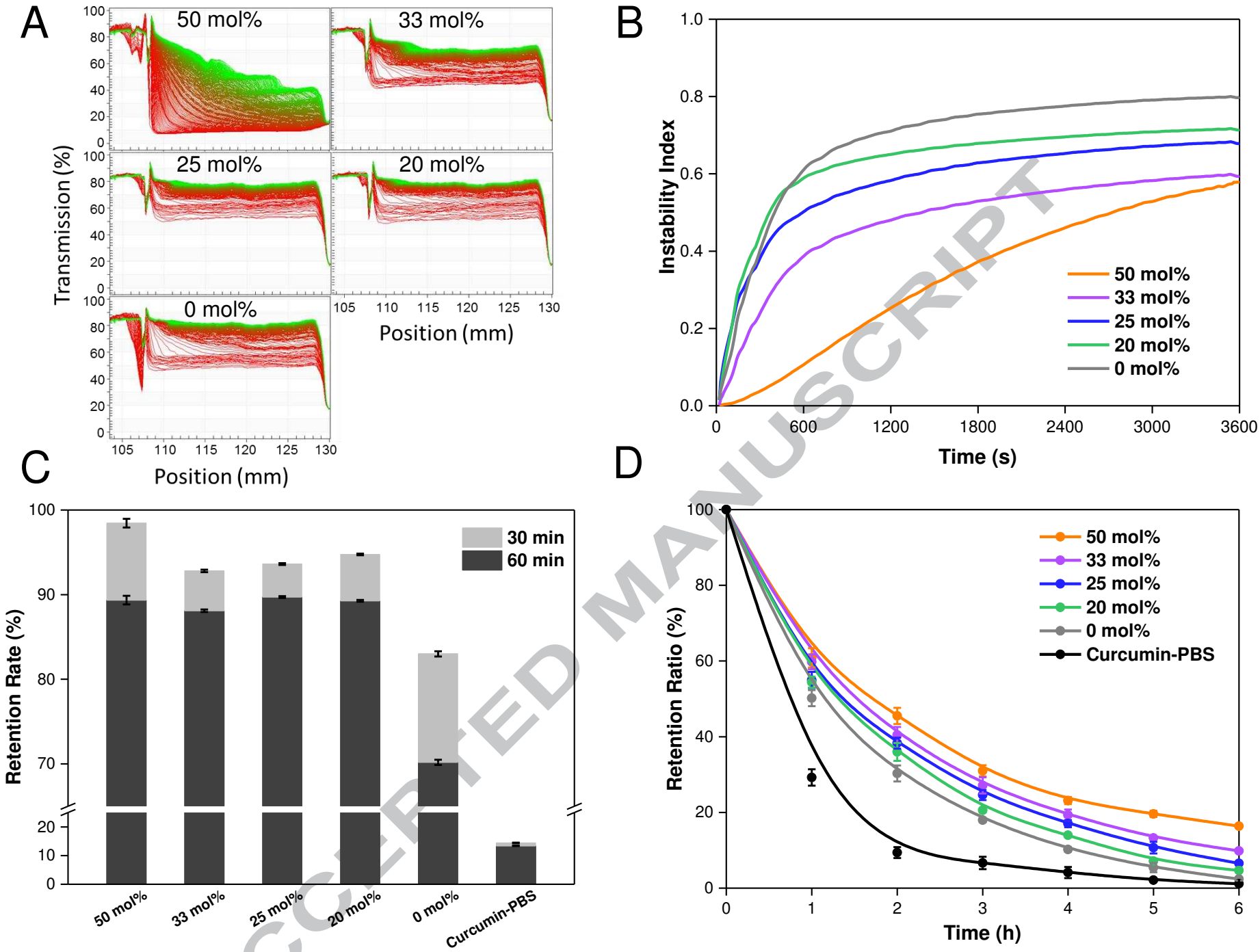

Fig. 3

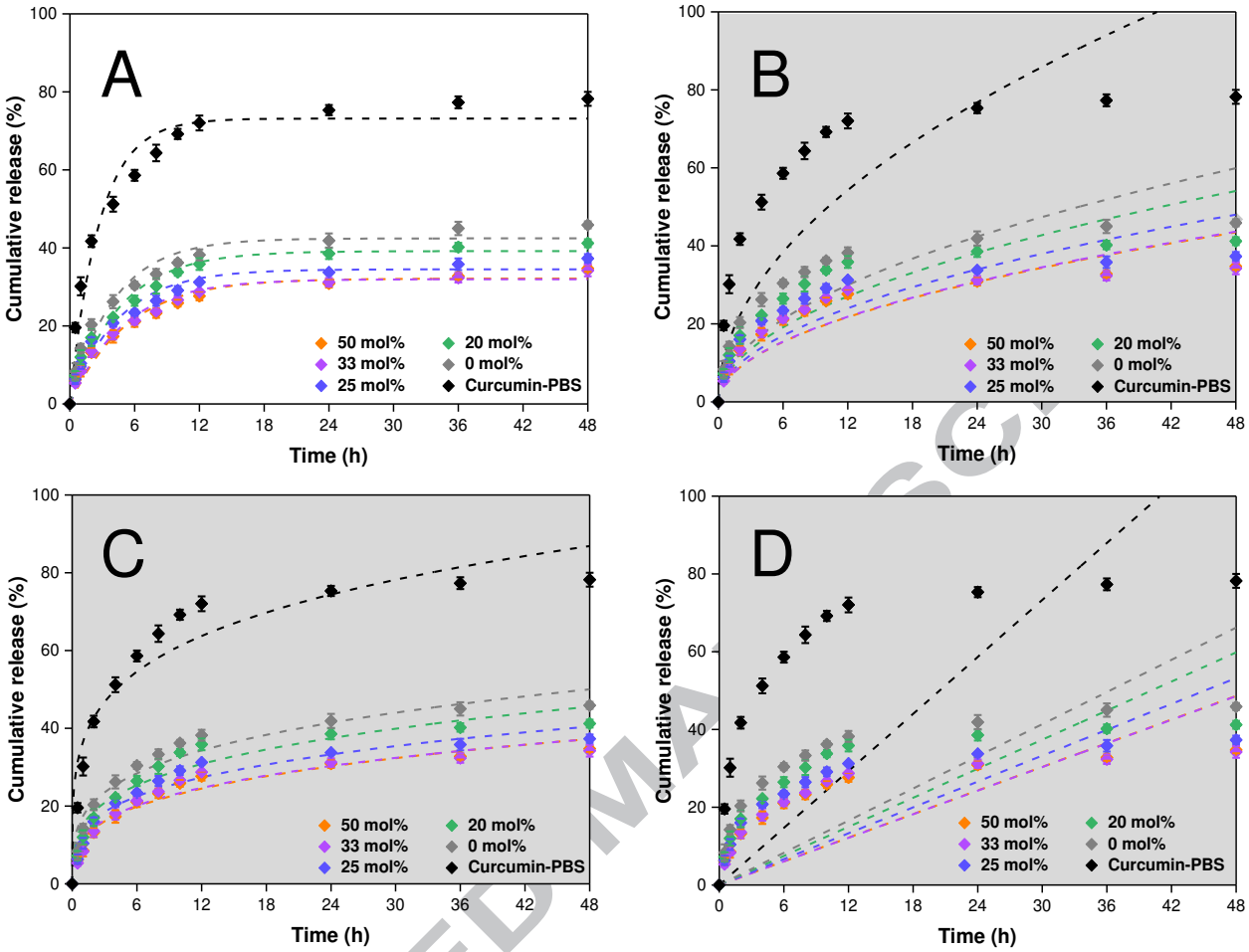

Fig. 4

Table Captions

Table 1. Results of vesicle size during storage time, encapsulation efficiency (EE) and bioavailability of curcumin-loaded liposomes with different concentration of β-sitosterol incorporated (mean ± standard deviation). Different letters (a-j, A-E, A′-C′) indicate significant differences for different Cur-LP specimens ($p < 0.05$).

Concentration of Sito (mol%)	Vesicle size (nm) during storage time (day)							EE (%)	Bioavailability (%
	0	1	2	4	7	14	21		
50	383±11^{f}	414±10^{gh}	408±14^{g}	422±5^{gh}	434±12^{hi}	446±8^{ij}	458±7^{j}	73.2±0.6^{A}	50.2±0.3$^{A'}$
33	194±4^{a}	198±5^{ab}	200±6^{ab}	194±4^{a}	203±1^{ab}	203±5^{ab}	206±1^{ab}	84.5±0.2^{E}	57.1±0.2$^{C'}$
25	197±2^{ab}	192±6^{a}	195±7^{ab}	192±9^{a}	200±2^{ab}	191±1^{ab}	210±15^{ab}	82.8±0.3^{D}	54.2±0.3$^{B'}$
20	197±4^{ab}	200±2^{ab}	189±4^{a}	201±10^{ab}	220±4^{bc}	203±12^{bc}	198±7^{ab}	81.5±0.2^{C}	53.9±0.3$^{B'}$
0	233±11^{c}	291±7^{d}	312±4^{e}	280±7^{d}	287±11^{d}	274±3^{d}	330±12^{e}	73.9±0.1^{B}	50.3±0.3$^{A'}$

Table 2. Fitted equations, correlation coefficients (R^2) and standard error (SE) obtained from the application of four kinds of release kinetic models.

Samples	Release kinetic models			
	Zero-order	**First-order**	**Higuchi**	**Ritger-Peppas**
50 mol%	**$M_t / M_0 = 1.013 \cdot t$** R^2=0.7234 SE=0.1780	**$M_t / M_0 = 32.147 \cdot (1-\exp(-0.189 \cdot t))$** R^2=0.9643 SE=0.0222	**$M_t / M_0 = 6.272 \cdot t^{1/2}$** R^2=0.7940 SE=0.4130	**$M_t / M_0 = 11.526 \cdot t^{0.303}$** R^2=0.9600 SE=0.0269
33 mol%	**$M_t / M_0 = 1.012 \cdot t$** R^2=0.7074 SE=0.1847	**$M_t / M_0 = 31.978 \cdot (1-\exp(-0.203 \cdot t))$** R^2=0.9750 SE=0.0202	**$M_t / M_0 = 6.300 \cdot t^{1/2}$** R^2=0.7602 SE=0.4506	**$M_t / M_0 = 11.824 \cdot t^{0.296}$** R^2=0.9483 SE=0.0328
25 mol%	**$M_t / M_0 = 1.109 \cdot t$** R^2=0.6985 SE=0.2066	**$M_t / M_0 = 34.520 \cdot (1-\exp(-0.224 \cdot t))$** R^2=0.9623 SE=0.0277	**$M_t / M_0 = 6.931 \cdot t^{1/2}$** R^2=0.7279 SE=0.5140	**$M_t / M_0 = 13.563 \cdot t^{0.282}$** R^2=0.9402 SE=0.0291
20 mol%	**$M_t / M_0 = 1.246 \cdot t$** R^2=0.6923 SE=0.2355	**$M_t / M_0 = 39.182 \cdot (1-\exp(-0.218 \cdot t))$** R^2=0.9712 SE=0.235	**$M_t / M_0 = 7.805 \cdot t^{1/2}$** R^2=0.7170 SE=0.5948	**$M_t / M_0 = 15.295 \cdot t^{0.282}$** R^2=0.9366 SE=0.0325
0 mol%	**$M_t / M_0 = 1.379 \cdot t$** R^2=0.6898 SE=0.2621	**$M_t / M_0 = 42.440 \cdot (1-\exp(-0.243 \cdot t))$** R^2=0.9565 SE=0.0326	**$M_t / M_0 = 8.647 \cdot t^{1/2}$** R^2=0.6970 SE=0.6645	**$M_t / M_0 = 17.459 \cdot t^{0.272}$** R^2=0.9517 SE=0.0273
Curcumin-PBS	**$M_t / M_0 = 2.443 \cdot t$** R^2=0.6309 SE=0.5868	**$M_t / M_0 = 73.154 \cdot (1-\exp(-0.368 \cdot t))$** R^2=0.9582 SE=0.0499	**$M_t / M_0 = 15.671 \cdot t^{1/2}$** R^2=0.4677 SE=1.5048	**$M_t / M_0 = 36.575 \cdot t^{0.223}$** R^2=0.9282 SE=0.0293

Highlights

1. The incorporation of β-sitosterol improved the encapsulation of curcumin.
2. Stability was improved when β-sitosterol was inserted into curcumin liposomes.
3. First-order model was fit for curcumin release from β-sitosterol liposomes.
4. The more β-sitosterol slowed the release of curcumin from liposomes better.
5. Bioavailability of curcumin was improved for β-sitosterol liposomes.